Establishment of a three-dimensional triculture model on the novel AXTEX-4D™ platform

AMBICA BARU, SAUMYABRATA MAZUMDER, PRABUDDHA KUNDU, SWATI SHARMA, BISWA PRATIM DAS PURAKAYASTHA, SAMEENA KHAN, REESHU GUPTA and NUPUR MEHROTRA ARORA

Mammalian Cell Culture Lab, Premas Biotech Pvt Ltd., Imt Manesar, Gurgaon 122050, India

Received May 4, 2022; Accepted August 31, 2022

DOI: 10.3892/or.2022.8439

Abstract. Cancer can be fatal if it is not treated in a timely manner; therefore, there is a high demand for more specific oncology drugs. Unfortunately, drugs showing positive responses on a two-dimensional (2D) culture platform do not often show the same effect in clinical trials. Therefore, three-dimensional (3D) culture platforms are garnering attention since they more closely mimic the tumor microenvironment (TME). The TME stimulates metastasis and drug resistance, and serves an essential role in tumor formation. An accurate understanding of tumor-stroma interactions is undoubtedly required to improve the response of patients to therapeutic strategies, and cancer therapeutic strategies that do not account for the stroma are considered inadequate. It should be noted that 3D monoculture systems do not completely mimic the TME since other cells in the 3D culture are missing, such as fibroblast or endothelial cells, which are essential components of the stroma; therefore, it is essential to develop advanced 3D culture systems. The present study aimed to develop a versatile triculture model that mimics the native TME; therefore, it could aid in high-throughput screening of chemotherapeutic drugs against cancer by evaluating their effects on tumor progression and cell cytotoxicity. The present study demonstrated the use of the AXTEX-4D™ platform in developing triculture tissueoids composed of MCF-7, human umbilical vein endothelial cells and MRC5 cells, and compared it with a 3D monoculture model (MCF-7) and a 2D culture model. The triculture model was validated for proliferation, ECM markers and T-cell infiltration by confocal microscopy. Alamar Blue assay demonstrated that triculture tissueoids exhibited higher drug resistance than the other two models, thus demonstrating their use in the screening of oncology drugs.

Correspondence to: Dr Nupur Mehrotra Arora, Mammalian Cell Culture Lab, Premas Biotech Pvt Ltd., Plot 77, Sector 4, Imt Manesar, Gurgaon 122050, India
E-mail: reeshu.gupta@premasbiotech.com

Key words: AXTEX-4D™, triculture, cell cytotoxicity, anticancer agents

Introduction

Two-dimensional (2D) cell cultures have an important role in assessing drugs due to their simplicity, robustness, rapidity and cost-effectiveness. The elimination of several anticancer drugs during clinical development is often due to the overestimation of their anticancer activity on a 2D-culture-based screening platform. Considerable data have suggested the significance of three-dimensional (3D) cell culture systems over 2D culture systems, due to their ability to better mimic the actual tumor microenvironment (TME) (1). The transcriptional profiling of several genes and limited signal transduction pathways, including hypoxia, TGF, Wnt and epithelial-mesenchymal transition pathways, in 3D culture systems have shown similarities with tumor xenografts and patients with cancer (2,3). These data indicated that 3D culture systems may reduce the number of animal models required in drug screening and the failure rates of clinical trials.

The stroma is considered a critical component of the TME, which markedly affects numerous hallmarks of cancer (4). The tumor stroma is essential in various molecular processes that aid cancer progression, metastasis and tumor cell resistance to therapeutic drugs. An accurate understanding of tumor-stroma interactions may result in more effective ameliorative strategies, ultimately improving patient health outcomes. Cancer therapeutic strategies that do not account for the stroma are inadequate (4); this is one of the main reasons for the non-performance of a number of oncology drugs in clinical trials, irrespective of their high efficiency in 2D-cultured cell line-based models. Notably, only 6.7% of drugs are approved during their transition from the preclinical phase to phase I clinical trials (5). In addition, most drugs fail in phase III clinical trials, which is considered to be the most expensive phase of clinical trials. It should be noted that the median cost of phase I clinical trials is ~$3.4 million. By contrast, single phase II and III clinical trials cost ~$8.6 and $19 million, respectively (6,7). One of the most challenging oncology issues is the problem of developing productive drugs in a time-saving and economical manner. Therefore, there is an urgent need for the development of cost- and time-efficient platforms for the screening of therapeutic drugs.

Various 3D innovative technologies are currently available, which have advanced the screening of antitumor agents, such as magnetic levitation, gel embedding technologies, 3D

bioprinting and microfluidic cell culture. In the magnetic levitation procedure, magnetic forces are applied to deliver magnetic nanoparticles to 2D cells, which help in forming 3D spheroids by making physiologically relevant extracellular matrix (ECM) (8). In the gel embedding technology, a hydrophilic polymer-based gel is used to form a 3D spheroid-like structure; this 3D structure facilitates cell-cell/cell-ECM interaction and supports signaling involved in inducing drug resistance of cancer cells (9). Although 3D culture systems have received attention over 2D culture systems, they lack the interactions of tumor cells with other cells of the stroma, such as fibroblasts or endothelial cells. Therefore, these 3D systems cannot mimic the TME. Co-culture of tumor cells with other cells of the stroma could be a partial solution to issues related with the failure of oncology drugs in clinical trials. Therefore, there is an urgent need to develop advanced 3D culture platforms for drug screening (10).

The present study developed a 3D triculture model using epithelial MCF-7 cells, fibroblast MRC5 cells and human umbilical vein endothelial cells (HUVECs) embedded in the AXTEX-4D™ platform. Briefly, the AXTEX-4D is a platform composed of a nonwoven fabric base matrix (polyethylene terephthalate) that receives and supports the growth of tissueoids. These polymers are less prone to heat and stress, making them autoclavable and capable of providing mechanical strength. In addition, the size of pores in the platform is 65 mm, which is designed to sustain cell adhesion and cell morphology. The present study also explored the use of the triculture model in testing the action of chemotherapeutic drugs in solid cancers compared with 3D monoculture and 2D culture models.

Materials and methods

Materials. The anti-collagen I (cat. no. AB745) and anti-laminin antibodies (cat. no. L8271) were purchased from MilliporeSigma. Anti-Ki67 antibodies were purchased from Abcam (cat. no. ab15580). Anti-mouse Alexa Fluor® 594-conjugated secondary antibodies (cat. no. A11005; 1:1,000) were purchased from Thermo Fisher Scientific, Inc., and anti-rabbit Alexa Fluor 488-conjugated secondary antibodies (cat. no. ab150077; 1:1,000) were obtained from Abcam. CFSE Blue (cat. no. C34574) and CFSE Green (cat. no. C34554) dyes were from Invitrogen; Thermo Fisher Scientific, Inc. Dil Red (cat. no. D3911) dye was obtained from Thermo Fisher Scientific, Inc. CFSE Blue, CFSE Green and Dil Red were used to stain the tumor cells (MCF-7 and HT-29), HUVECs and MRC5 cells, respectively.

Cell lines. Human breast cancer MCF-7 cells, colorectal cancer HT-29 cells, HUVECs (passage 1; CRL-1730™) and human lung fibroblast MRC-5 cells were obtained from ATCC. EMEM (MilliporeSigma) was used to culture MCF-7, HT-29 and MRC-5 cells, whereas HUVECs and Jurkat T cells (TIB-152™; ATCC) were cultured in EBM2 (Lonza Group Ltd.) and RPMI-1640 (MilliporeSigma), respectively. All media were supplemented with 10% FBS (Gibco; Thermo Fisher Scientific, Inc.) and 2 mM glutamine (MilliporeSigma). Cells were cultured at 37˚C and 8% CO_2 was supplied to cells under static conditions. Two tumor cell lines (MCF-7 and HT-29) were used to show the versality of the AXTEX-4D platform.

Establishing 3D monocultures and tricultures

3D monoculture and triculture tissueoids on the AXTEX-4D. The AXTEX-4D platform (Premas Biotech Pvt Ltd.) was used to form 3D tissueoids as described previously (7,11,12). A patent for the platform has been filed (patent no. US 20200326330 A1; application filed, January 29, 2020; publication date, October 15, 2020) by Premas Biotech Pvt Ltd. The platform is in the exploratory phase and currently has no catalogue number. For 3D monoculture tissueoids, 5,000 MCF-7 cells were used; for 3D triculture tissueoids, a suspension of the MCF-7 cell line was mixed with MRC-5 and HUVEC cell lines in a 1:2:1 ratio (1,250 tumor cells, 2,500 fibroblast cells and 1,250 endothelial cells). The cell population was used to make monoculture and triculture tissueoids on the platform and further used for various experiments. Briefly, ~$0.8x10^6$ cells (monoculture and triculture) were seeded in 60-mm dish and were allowed to grow until 70-80% confluence was reached. Cells were then washed and centrifuged at 120 x g for 5 min at room temperature. Finally, a cell suspension was generated so that each drop of media contained 5,000 cells. A single drop of media containing 5,000 cells was used to make 3D tissueoids on the AXTEX-4D platform and underwent subsequent experiments.

To evaluate interactions among tumor cells, endothelial cells (HUVECs) and fibroblast cells (MRC5), MCF-7 and HT-29 tumor cells were grown as a monoculture and as tricultures on the AXTEX-4D platform for 4 days, since the HUVEC network would not last beyond the 7-day time point (13). 3D MCF-7 or HT-29 tissueoids were labelled with a blue fluorescence dye, whereas HUVECs and MRC5 cells were labelled with green and red fluorescence dyes, respectively. The localization of all of the three cell types was visualized via bright field or confocal microscopy and were visually assessed.

Proliferation and ECM formation. 3D monoculture and triculture tissueoids were stained with specific antibodies to assess proliferation and ECM formation. Briefly, tissueoids were formed on the AXTEX-4D platform after 24 h of culture and subsequently fixed with 4% paraformaldehyde for 15 min at room temperature, followed by washing with 1X PBS. Subsequently, permeabilization was performed with 0.1% Triton-X for 4 min at room temperature. After permeabilization, samples were blocked with 1% BSA (MilliporeSigma) for 1 h at room temperature, and were then incubated with anti-Ki67, anti-laminin and anti-collagen I antibodies (1:1,000, 1:500 and 1:50, respectively) overnight at 4˚C. Finally, tissueoids were incubated at 37˚C for 2 h with Alexa Fluor 488-conjugated anti-rabbit secondary antibodies (for Ki67 and collagen I; 1:1,000) and Alexa Fluor 594-conjugated anti-mouse secondary antibodies (for laminin; 1:1,000), and were washed with PBS. Tissueoids were counterstained with Hoechst and mounted using Prolong Gold mounting media. Imaging was then performed using a Leica TCS SP8 confocal microscope (Leica Microsystems, Inc.).

Tumor immune infiltration. Triculture tissueoids of breast cancer cells were generated after 24 h of culture on the AXTEX-4D platform. Briefly, 100 μl Jurkat cells ($5x10^4$ cells) were poured on the upper chamber of a Transwell system (Corning™ HTS Transwell®-96 Tissue Culture System; cat.

no. 3387; Corning, Inc.). Jurkat cells were stained with CFSE at 37˚C for 20 min and a chemoattractant (SDF1α or 10% FBS; Shenandoah Biotechnology, Inc.) was added to the lower chamber containing triculture tissueoids. The infiltration assay was performed as described previously by our group. The experiment was repeated three times, and one tissueoid per well was used to count T cells during each repeat. Images were captured using a Nikon confocal microscope (A1R HD25; Nikon Corp.) at x10 objective. The Cell Counter plug-in (version-2) of ImageJ (National Institutes of Health) was used to count the infiltrated T cells (14). First, channels were split using ImageJ. Using the 3D-OC set measurements, the cell measurements were set with dot and font size of 20. Subsequently, cells present on the edges were excluded and the background staining was minimized using a size filter. The number of cells was then quantified.

Alamar Blue assay. Tissueoids were formed after 24 h of culture on the AXTEX-4D platform and were subsequently treated with drugs. Briefly the 3D monoculture, triculture and 2D culture of MCF-7 breast cancer cells were treated with different concentrations of raloxifene (1, 10, 50 and 100 μM; cat. no. R0109; Tokyo Chemical Industry Co., Ltd.) and doxorubicin (2.5, 5 and 10 μM; MilliporeSigma) for 48 h at 37˚C. Subsequently, 20 μl Alamar Blue solution (cat. no. DAL1025; Invitrogen; Thermo Fisher Scientific, Inc.) was directly added to 200 μl medium and the cells were incubated for 4 h at 37˚C. The Alamar Blue assay was performed as described previously (15). An ELISA plate reader (Spectramax Gemini EM; Molecular Devices, LLC) was used to determine relative fluorescence units (RFU). The following formula was used to calculate cell viability (15): Viability (%)=RFU value of cells treated with raloxifene/RFU value of the control untreated cells x100.

Statistical analysis. Each experiment was repeated three times and results are presented as the mean ± SEM. The difference in cell viability was assessed using one-way analysis of variance followed by Bonferroni-post hoc test. OriginPro (Version:2020b) (Konark solutions Bangalore Private Limited) was used for all statistical analyses. P£0.05 was considered to indicate a statistically significant difference.

Results

Establishing a triculture tissueoid model using the AXTEX 4D platform. When two or more cell populations are used together to develop a co-culture model, they co-exist together (16). However, in the native environment, several phenotypically distinct cells exist together near to each other or in a more compact organizational form and exert strong paracrine effects (17). Proliferation of solid cancer cells along with HUVECs and MRC5 cells resulted in the formation of MCF-7 and HT-29 cell triculture tissueoids (Figs. 1 and 2). It is evident that all three cells could co-exist together in the triculture model.

Study of cellular proliferation and ECM interactions in cancer tissueoids. The aim of the present study was to develop a versatile triculture model that could be used for the screening of chemotherapeutic drugs with high efficiency against cancer by evaluating their effects on tumor progression and cell cytotoxicity. The expression of Ki67 (a marker of proliferation) and ECM formation are strongly associated with tumor cell proliferation, tumor progression, survival and therapeutic resistance in the tumor microenvironment. Therefore, they are widely used in routine screening of chemotherapeutic drugs (18-21). Ki67 immunostaining (Fig. 3A and B) indicated that MCF-7 triculture tissueoids displayed a homogeneous distribution pattern of Ki67-positive cells, whereas Ki67 staining was mostly restricted to the outmost cell layers in MCF-7 monoculture tissueoids (Fig. 3A). In contrast to MCF-7 cells, HT-29 monoculture and triculture tissueoids displayed homogenous distribution of Ki67-positive cells, indicating that different cancer cell types exhibit different cellular organization in their native environment (Fig. 3B).

Collagens and laminins are the main component of the ECM, which provide structural support, and regulate cell attachment, migration and differentiation. These components promote tissue repair and modulate cellular behavior (22,23). The interaction of collagen and laminin is expected to be essential for ECM formation; however, little work has been done to study the interactions (24). In the present study, strong signals were detected for laminin in the innermost region of MCF-7 monoculture and triculture tissueoids, whereas collagen was detected in the outermost region in the case of MCF-7 monoculture and triculture tissueoids (Fig. 4A). In HT-29 monoculture and triculture tissueoids, collagen and laminin signals were detected throughout the tissueoid (Fig. 4B). These results suggested no visible interconnection between collagen and laminin in the MCF-7 3D tissueoids; however, it was visible in both monoculture and triculture 3D tissueoids of HT-29 cells (Fig. 4B), suggesting the strong structural support of the cells. However, further investigation is essential to confirm these findings.

Infiltration of Jurkat T cells in triculture model. The identification of drugs that manipulate the interaction of immune system cells, fibroblasts and endothelial cells with tumor cells may lead to novel cancer treatments (25). Our previous study explored the infiltration of T cells in a monoculture tissueoid model (11). Using the same strategy in the present study, the infiltration of immune T cells was investigated in the triculture model. Confocal microscopy revealed the significant infiltration of Jurkat T cells in the 3D MCF-7 triculture tissueoids in the presence of both 10% FBS and SDF-1a in comparison to unstimulated cells (Fig. 5). However, T-cell infiltration was not obvious in the unstimulated (0% FBS) 3D triculture tissueoid model. The results were similar to those detected in the monoculture tissueoids in our previous study (11).

Drug sensitivity in 2D culture, and 3D monoculture and triculture. The lack of interactions between tumor cells and stromal tissues or blood flow through endothelial cells in a 3D culture model make them unable to completely mimic the TME. Previous studies have shown greater clinical relevance of 3D tricultures, due to their enhanced resistance to chemotherapeutics, compared with 2D cultures (26,27). To this end, the present study evaluated drug sensitivity in a 2D culture, and in 3D

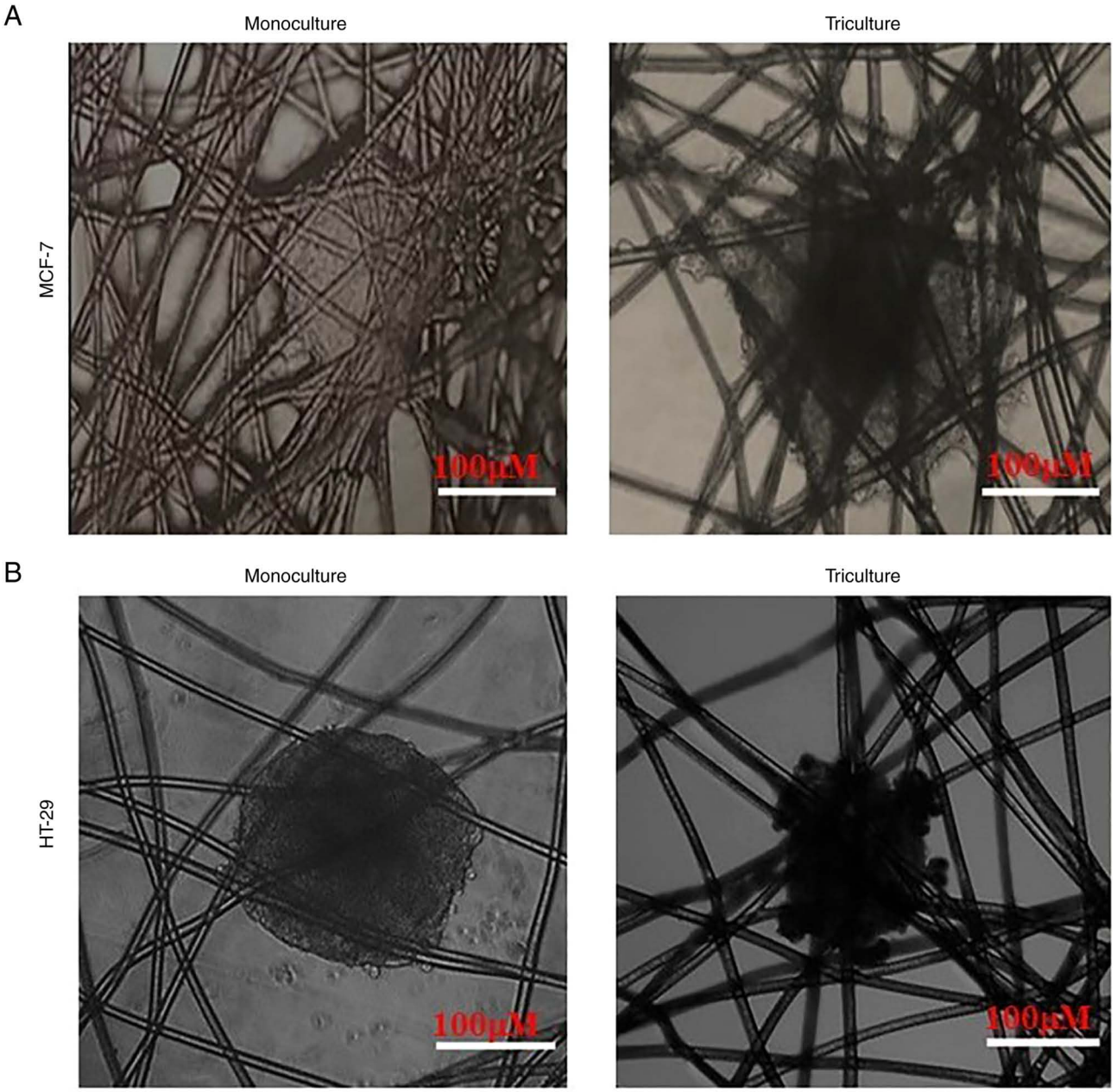

Figure 1. Triculture model of solid cancer tissueoids on the AXTEX-4D™ platform (11). Bright field microscopy images of (A) MCF-7 and (B) HT-29 tissueoids. Monoculture (left panel) and triculture (right panel) of (A) MCF-7 and (B) HT-29 tissueoids with MRC-5 (fibroblasts) and human umbilical vein endothelial cells after 2 days in a 1:2:1 ratio.

monoculture and tricultures tissueoids of MCF-7 cells by Alamar Blue assay to demonstrate drug-induced cytotoxicity (Fig. 6). Breast cancer 3D tricultures and monocultures were treated with different doses of raloxifene (1, 10, 50 and 100 μM) and were compared with 2D monocultures for 48 h. Compared with the 3D tricultures, MCF-7 cells cultured in 2D and 3D monocultures exhibited reduced cellular viability following raloxifene treatment. The percentages of cell viability following raloxifene treatment were as follows: 3D triculture, 1 μM, 107.01±19.81%; 10 μM, 190.23±21.13%; 50 μM, 179.12±32.62%; 100 μM, 20.31±8.50%. 3D monoculture, 1 μM, 101.05±2.26%; 10 μM, 85.05±0.46%; 50 μM, 69.13±1.05%, 100 μM, 15.19±0.16%. 2D culture, 1 μM, 69.06±10.41%; 10 μM, 73.18±7.73%; 50 μM, 4.71±1.32%; 100 μM, 4.63±1.92% (Fig. 6A).

Similar results were obtained using doxorubicin (Fig. 6B). The maximum serum concentration achievable for doxorubicin is 6.73 μM (28); therefore, breast cancer 3D tricultures and monocultures were treated with different doses of doxorubicin (2.5, 5 and 10 μM) and compared with 2D monocultures for 48 h. Compared with the 3D tricultures, both 2D cultures and 3D monocultures of breast cancer cells were most sensitive to the drug doses applied. The percentages of cell viability following doxorubicin treatment were as follows: 3D triculture, 2.5 μM, 99.81±0.18%; 5 μM, 99.45±0.48%; 10 μM, 98.71±0.74%. 3D monoculture, 2.5 μM, 99.75±0.18%; 5 μM, 97.50±1.88%; 10 μM, 86.73±8.88%. 2D culture, 2.5 μM, 55.03± 33%; 5 μM, 48.12±28%; 10 μM, 23.14±13% (Fig. 6B). These results suggested that MCF-7 3D tricultures and monocultures were

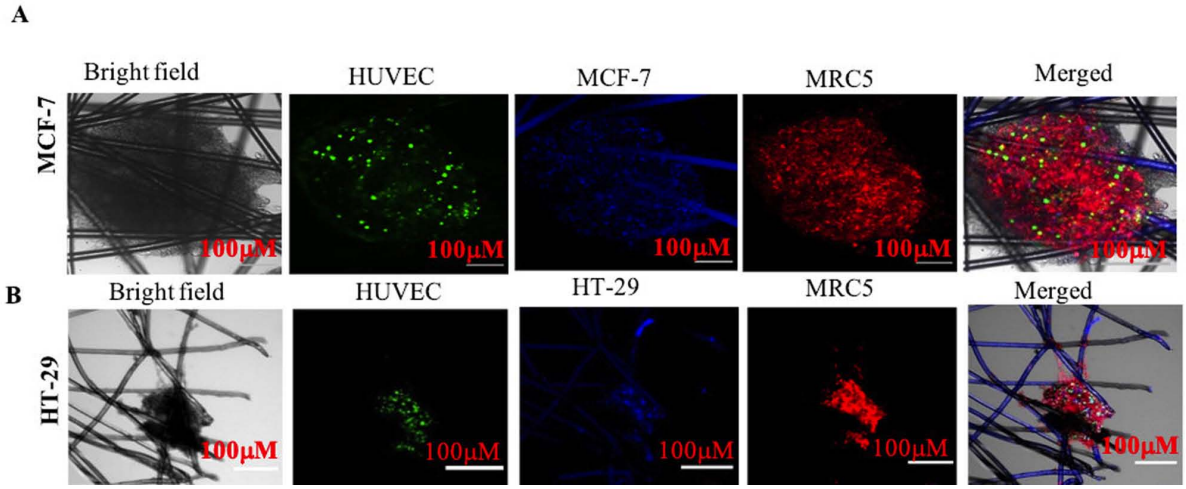

Figure 2. Confocal microscopy of a triculture model of solid cancer tissueoids on the AXTEX-4D™ platform. (A) MCF-7 and (B) HT-29 triculture tissueoids (blue) depicting MRC5 cell (red) and HUVECs (green). HUVECs, human umbilical vein endothelial cells.

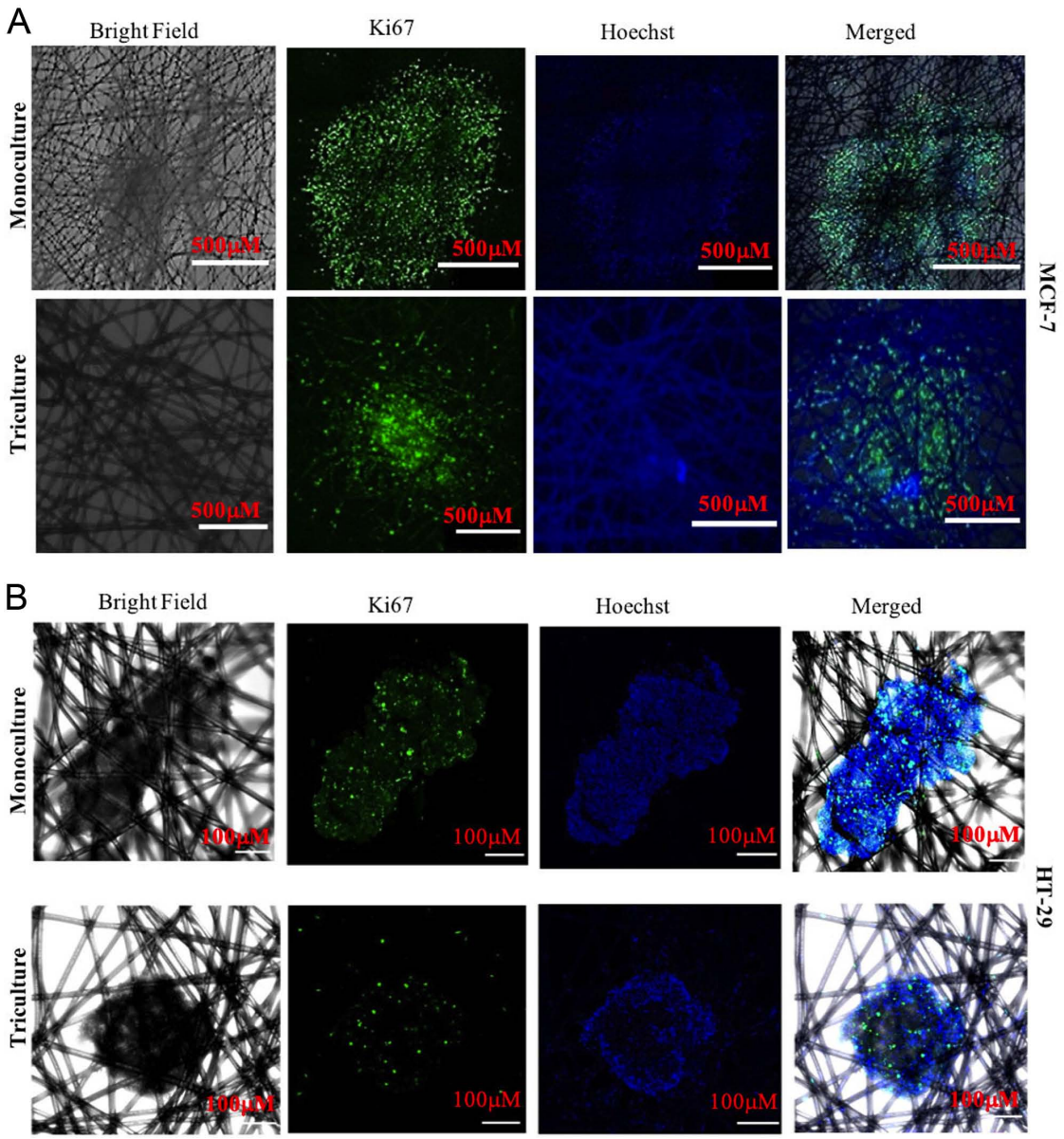

Figure 3. Proliferation of MCF-7 and HT-29 tissueoids on the AXTEX-4D™ platform. Monocultures (upper panel) and tricultures (lower panel) of (A) MCF-7 and (B) HT-29 tissueoids were grown on the AXTEX-4D platform for 7 days. The cells were stained with anti-Ki67 antibody.

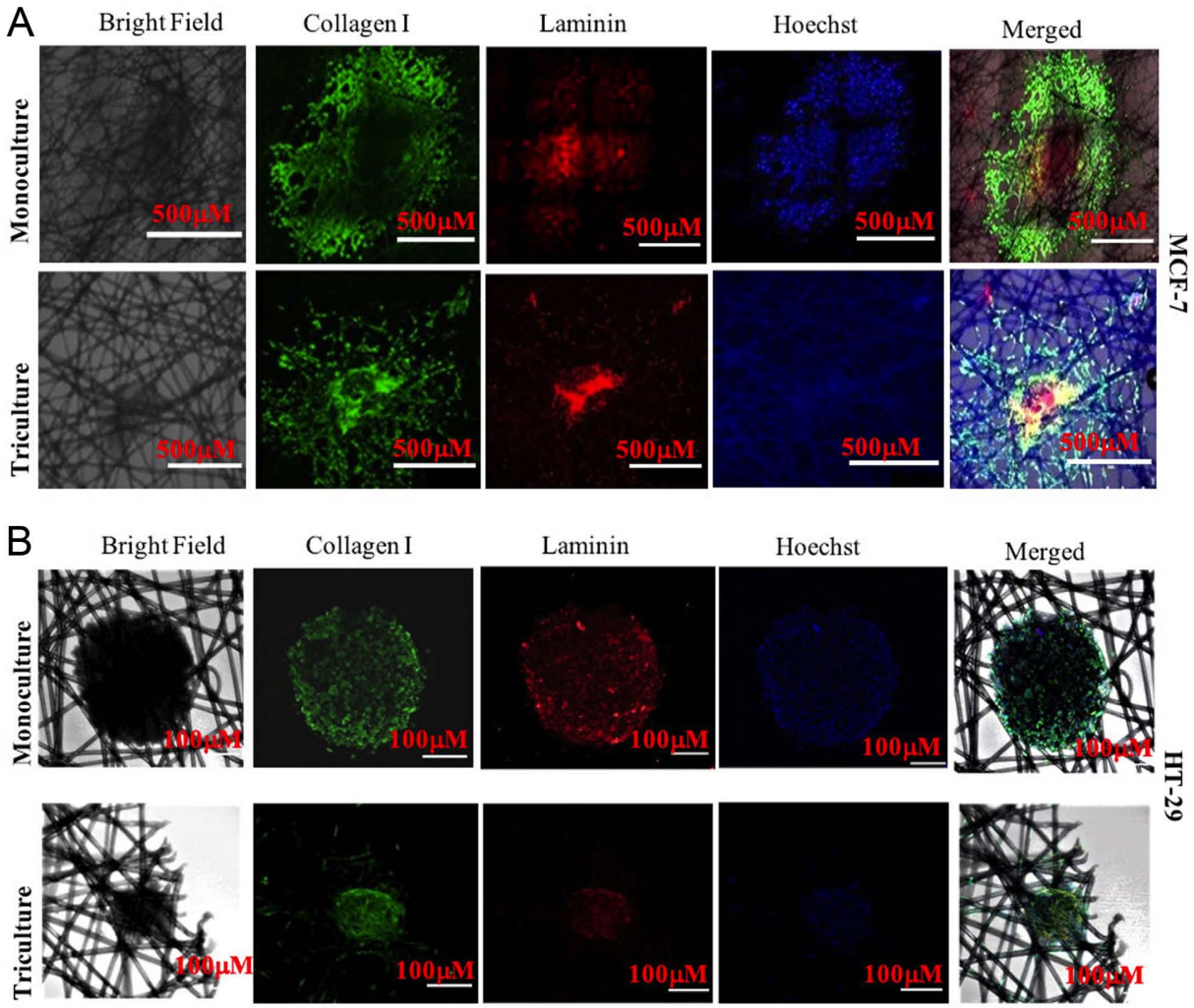

Figure 4. Extracellular matrix formation in MCF-7 and HT-29 tissueoids on the AXTEX-4D™ platform. Monocultures (upper panel) and tricultures (lower panel) of (A) MCF-7 and (B) HT-29 tissueoids were grown on the AXTEX-4D platform for 7 days. The cells were stained with anti-collagen I and anti-laminin.

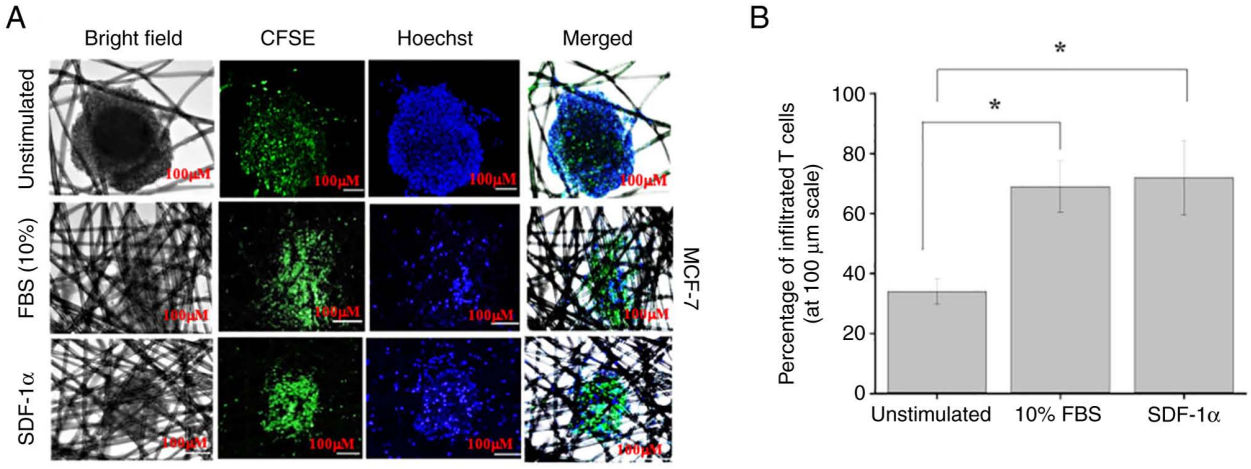

Figure 5. Infiltration of Jurkat T cells (immune cells) towards breast cancer tissueoids. (A) MCF-7 tissueoids tricultures were co-cultured with Jurkat T-cells and stained with Hoechst dye (blue). Jurkat T cells (green) were stained with CFSE green. (B) Quantification of T-cell infiltration was performed by Fiji distribution using ImageJ software. The experiment was repeated three times. *P<0.05.

significantly more resistant to raloxifene and doxorubicin than 2D cultures, with the triculture showing maximum drug resistance. Xenograft models of MCF-7 tumors have been shown to exhibit drug resistance (29-32). These results suggested that the response to anticancer drugs in the 3D triculture and monoculture systems was more similar to the response observed for

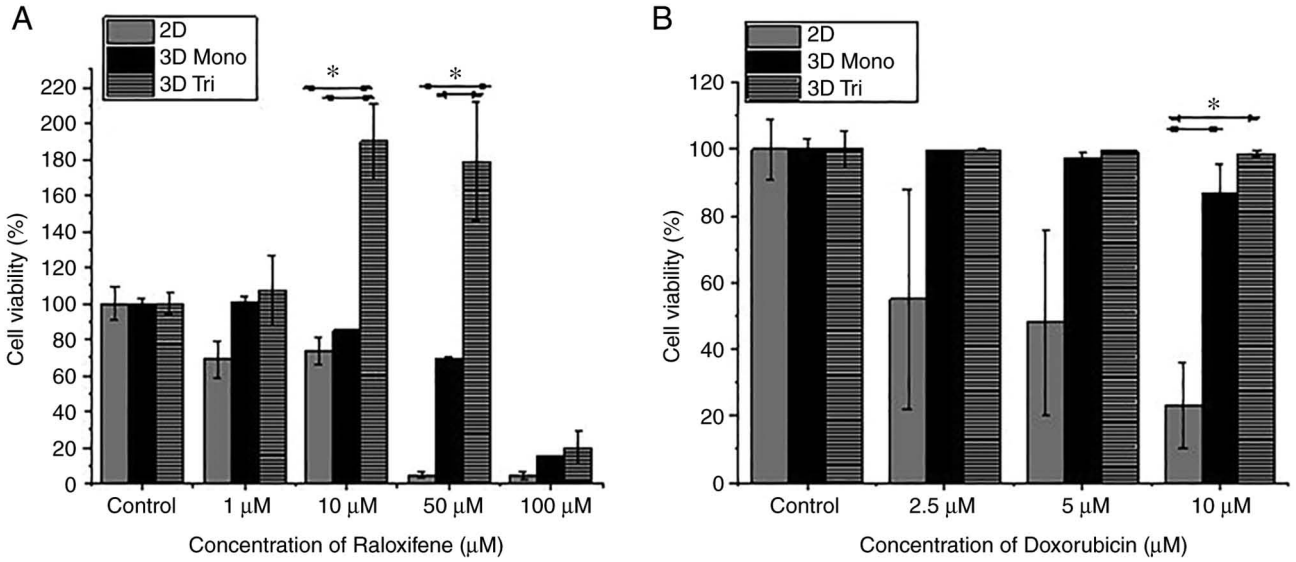

Figure 6. Effect of chemotherapeutic drugs on cytotoxicity in 2D culture, 3D monoculture and 3D triculture models. MCF-7 cells were grown as 2D, 3D monoculture and 3D triculture, and were treated with the indicated doses of (A) raloxifene and (B) doxorubicin for 48 h. Cell viability was determined using Alamar Blue assay. Data are presented as the mean ± SEM. *P≤0.05. 2D, two-dimensional; 3D, three-dimensional.

the same drugs in xenograft models; however, it is not true in the case of the 2D culture systems. These results further suggested that the developed 3D monoculture and triculture models may regulate mechanisms associated with the drug resistance of tumor cells, such as mechanisms associated with drug inactivation, multi-drug resistance, cell death inhibition, DNA-repair and target gene amplification and may be used to assess mechanisms associated with drug resistance (33).

Discussion

The present study developed a triculture tissueoid model containing endothelial cells, fibroblasts and tumor cells on the AXTEX-4D platform, which mimics the TME. The TME in solid tumors not only contains tumor cells but also contains endothelial cells, ECM, stromal cells and immune cells, which are an essential and larger part of the tumor mass. Interactions among tumor, vascular and other cells promotes cancer growth through cell-cell and ECM interactions (34-36). Previous studies have also shown the role of direct interaction of cancer cells with fibroblasts and/or vascular cells in cancer cell invasion and metastasis (37,38). The present study demonstrated the utility of the AXTEX-4D platform in developing a triculture tissueoid model that may be used in studying tumor, vascular and fibroblast cell interactions, which serve an essential role in tumor growth, metastasis, and the evaluation of anti-angiogenic and vascular targeting therapies. Additionally, the ability of the AXTEX-4D platform in evaluating the expression of proliferative markers and ECM formation, which may control the tumor response toward therapy, was assessed. Although the present study demonstrated the importance of the developed triculture model in assessing tumor-related characteristics, further investigations at the molecular level to measure the difference in the expression levels of tumor markers are necessary.

The ECM is associated with numerous factors, such as tissue stiffness, interactions with relevant receptors and tumor progression (39). The expression of laminin receptors, laminin, collagen, collagenase and Ki67 have been shown to be associated with pathological grade and the clinical behavior of tumors (40). Consistent with these studies, the present study observed the expression of Ki67, collagen I and laminin (ECM markers) in 3D monoculture and triculture tissueoids of MCF-7 and HT-29 cells. However, flow cytometric analysis of proliferative and ECM markers is required to confirm the statistical differences, which will be performed in our future studies. Notably, differences were observed in the localization of Ki67, collagen and laminin staining between monocultures and tricultures. As reported previously, the interaction of tumor cells with other cells in the stroma in the triculture model affects the image quality of confocal microscopy and results in a lower resolution, most likely due to altered compactness or different cell types (41-44) and could be the reason for the differences in the localization of Ki67 between the monoculture and triculture models. However, more experimental data are required to verify this. These results suggested that the tissueoid model may be used to evaluate and screen anticancer agents targeting proliferation and ECM formation, and may help study the therapeutic resistance of tumor cells.

The lack of interactions between tumor cells and stromal tissues or blood flow through endothelial cells in 3D culture models make them unable to completely mimic the TME. Several studies have demonstrated the drug resistance features of 3D models over 2D cultures (45,46). For example, the 3D culture of paclitaxel-treated ovarian cancer cells exhibited reduced cell death (40 or 60%) compared with the 2D culture (80%) (45). These results indicated that chemotherapeutic drugs have reduced activity in 3D culture models and may be associated with increased drug resistance. Limited diffusion through the spheroid, hypoxia and the presence of stromal cells are other factors that could contribute to drug resistance (47,48). Similar drug resistance as observed in 3D spheroids has also been observed *in vivo* (49,50). Similar to xenograft models, breast cancer spheroids have been shown to develop multi-lobular structures, wavy protrusions and drug

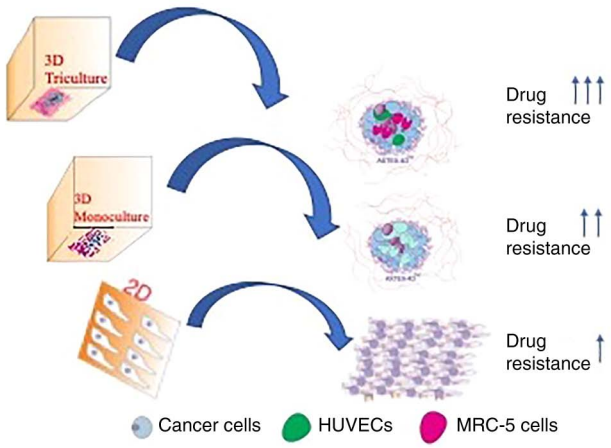

Figure 7. Graphical representation depicting the drug resistance of 2D, 3D monoculture and 3D triculture tissueoids. HUVECs, human umbilical vein endothelial cells.

resistance (51). However, the triculture models, compared with 2D culture models, provide a physiologically relevant model for assessing cancer cell growth, drug response and therapeutic screening (27,51,52). The present study demonstrated higher drug resistance to raloxifene and doxorubicin in the triculture tissueoids compared with in the 3D monoculture and 2D culture models. However, it should be noted that in contrast to raloxifene, doxorubicin is a DNA topoisomerase II inhibitor that is not applied for the treatment of ERa-positive breast cancer, such as MCF-7, which show resistance against doxorubicin treatment (53).

In the present study, cell cytotoxicity was observed using clinically achievable concentrations of drugs (28). These findings suggested that the use of a 3D culture model may avert the overestimation of drug efficacy. Increased cell viability was detected in response to every dose of raloxifene and doxorubicin in the triculture model compared with that in the monoculture model. Nevertheless, the absence of significant differences in cell viability in 3D monocultures compared with in 3D tricultures is an unpredicted observation and needs further refinement.

It was hypothesized that the triculture tissueoid model involving three different cell types will produce more clinically relevant results than 2D and 3D monocultures (Fig. 7). It should be noted that there are several advantages and limitations to the use of advanced 3D approaches in terms of analyzing information-rich biological data. For example, microfluidic cell culture has the advantage of more closely mimicking the TME, as in this system a continuous supply of media is provided to the culture. Other advantages include the requirement of a smaller number of cells and reagents, reduced risk of contamination and efficient high-speed experimentation; however, it is a complicated system that requires skills and a trained user (54). Sample retrieval is also difficult for further analysis. Magnetic levitation and gel embedding methodology also have several limitations, such as poor mechanical strength of cells and difficulty in performing immunohistochemistry for studying biomarkers (55). By contrast, AXTEX-4D is a simple, less expensive and user-friendly platform for performing downstream experiments, such as fluorescence microscopy, confocal microscopy and ELISA. However, the platform has several limitations, such as no continuous supply of media and removal of waste, thus limiting its automation capability (2). In addition, the present study did not perform downstream assays on patient-derived tumors, which is an important aspect of any cell culture platform (56-59). Therefore, further advancement of the model described in the present study is needed. We aim to refine our platform with patient-derived xenografts. Furthermore, the present study did not explore signaling pathways associated with drug resistance.

Acknowledgements

We acknowledge Mr. Manish Kumar (CSIR-Institute of Genomics and Integrative Biology, New Delhi) for helping in imaging of tissueoids. We also want to acknowledge Mr. Rajan (Regional Centre for Biotechnology, India) for their assistance in image analysis and Mr. Avijit Das (Premas Biotech Pvt Ltd.) for their critical discussion on the experimental study.

Funding

No funding was received.

Availability of data and materials

The datasets used and/or analyzed during the current study are available from the corresponding author on reasonable request.

Authors' contributions

AB and SS designed and planned the experiments, conducted the experiments, analyzed the results and wrote the manuscript. SM, SK and BPDP were responsible for concept design. PK studied the concept, designed the study, interpreted the data and provided scientific inputs. RG analyzed data and drafted the manuscript. NMA studied the concept, designed the study, interpreted the data and provided scientific inputs and drafted the manuscript. All authors read and approved the final manuscript. AB, NM and PK confirm the authenticity of all the raw data.

Ethics approval and consent to participate

Experiments on the HUVEC line used in the present study were carried out after approval from the Premas Ethics Committee.

Patient consent for publication

Not applicable.

Competing interests

All authors are employees of Premas Biotech Pvt Ltd. A patent for the AXTEX-4D platform has been filed (patent no. US 20200326330 A1; application filed, January 29, 2020; publication date, October 15, 2020) and is currently in the exploratory phase.

References

1. Kapałczyńska M, Kolenda T, Przybyła W, Zajączkowska M, Teresiak A, Filas V, Ibbs M, Bliźniak R, Łuczewski Ł and Lamperska K: 2D and 3D cell cultures-a comparison of different types of cancer cell cultures. Arch Med Sci 14: 910-919, 2018.
2. Boghaert ER, Lu X, Hessler PE, McGonigal TP, Oleksijew A, Mitten MJ, Foster-Duke K, Hickson JA, Santo VE, Brito C, *et al*: The volume of three-dimensional cultures of cancer cells in vitro influences transcriptional profile differences and similarities with monolayer cultures and xenografted tumors. Neoplasia 19: 695-706, 2017.
3. Hirschhaeuser F, Menne H, Dittfeld C, West J, Mueller-Klieser W and Kunz-Schughart LA: Multicellular tumor spheroids: An underestimated tool is catching up again. J Biotechnol 148: 3-15, 2010.
4. Valkenburg KC, de Groot AE and Pienta KJ: Targeting the tumour stroma to improve cancer therapy. Nat Rev Clin Oncol 15: 366-381, 2018.
5. Hay M, Thomas DW, Craighead JL, Economides C and Rosenthal J: Clinical development success rates for investigational drugs. Nat Biotechnol 32: 40-51, 2014.
6. Martin L, Hutchens M, Hawkins C and Radnov A: How much do clinical trials cost? Nat Rev Drug Discov 16: 381-382, 2017.
7. Baru A, Mazumder S, Kundu PK, Sharma S, Das Purkayastha BP, Khan S, Gupta R and Mehrotra Arora N: Recapitulating tumor microenvironment using AXTEX-4DTM for accelerating cancer research and drug screening. Asian Pac J Cancer Prev 23: 561-571, 2022.
8. Haisler WL, Timm DM, Gage JA, Tseng H, Killian TC and Souza GR: Three-dimensional cell culturing by magnetic levitation. Nat Protoc 8: 1940-1949, 2013.
9. Lv D, Hu Z, Lu L, Lu H and Xu X: Three-dimensional cell culture: A powerful tool in tumor research and drug discovery. Oncol Lett 14: 6999-7010, 2017.
10. Imamura Y, Mukohara T, Shimono Y, Funakoshi Y, Chayahara N, Toyoda M, Kiyota N, Takao S, Kono S, Nakatsura T and Minami H: Comparison of 2D- and 3D-culture models as drug-testing platforms in breast cancer. Oncol Rep 33: 1837-1843, 2015.
11. Baru A, Sharma S, Purakayastha BP, Khan S, Mazumdar S, Gupta R, Kundu PK and Arora NM: AXTEX-4D: A three-dimensional ex vivo platform for preclinical investigations of immunotherapy agents. Assay Drug Dev Technol 19: 361-372, 2021.
12. Baru A Mazumdar S, Kundu P, Sharma S, Purakayastha BP, Khan S, Gupta R and Arora NM: Recapitulating tumor microenvironment using preclinical 3D tissueoids model for accelerating cancer research and drug screening. bioRxiv: Dec 22, 2020 (Epub ahead of print).
13. Bray LJ, Secker C, Murekatete B, Sievers J, Binner M, Welzel PB and Werner C: Three-dimensional in vitro hydro- and cryogel-based cell-culture models for the study of breast-cancer metastasis to bone. Cancers (Basel) 10: 292, 2018.
14. Wu Y, Wu H, Zeng J, Pluimer B, Dong S, Xie X, Guo X, Ge T, Liang X, Feng S, *et al*: Mild traumatic brain injury induces microvascular injury and accelerates Alzheimer-like pathogenesis in mice. Acta Neuropathol Commun 9: 74, 2021.
15. Eilenberger C, Kratz SRA, Rothbauer M, Ehmoser EK, Ertl P and Küpcü S: Optimized alamarBlue assay protocol for drug dose-response determination of 3D tumor spheroids. MethodsX 5: 781-787, 2018.
16. Lazzari G, Nicolas V, Matsusaki M, Akashi M, Couvreur P and Mura S: Multicellular spheroid based on a triple co-culture: A novel 3D model to mimic pancreatic tumor complexity. Acta Biomater 78: 296-307, 2018.
17. Lamichhane SP, Arya N, Kohler E, Xiang S, Christensen J and Shastri VP: Recapitulating epithelial tumor microenvironment in vitro using three dimensional tri-culture of human epithelial, endothelial, and mesenchymal cells. BMC Cancer 16: 581, 2016.
18. Shah PP, Dupre TV, Siskind LJ and Beverly LJ: Common cytotoxic chemotherapeutics induce epithelial-mesenchymal transition (EMT) downstream of ER stress. Oncotarget 8: 22625-22639, 2017.
19. Bai C, Yang M, Fan Z, Li S, Gao T and Fang Z: Associations of chemo- and radio-resistant phenotypes with the gap junction, adhesion and extracellular matrix in a three-dimensional culture model of soft sarcoma. J Exp Clin Cancer Res 34: 58, 2015.
20. Senthebane DA, Jonker T, Rowe A, Thomford NE, Munro D, Dandara C, Wonkam A, Govender D, Calder B, Soares NC, *et al*: The role of tumor microenvironment in chemoresistance: 3D extracellular matrices as accomplices. Int J Mol Sci 19: 2861, 2018.
21. Ellis MJ, Suman VJ, Hoog J, Goncalves R, Sanati S, Creighton CJ, DeSchryver K, Crouch E, Brink A, Watson M, *et al*: Ki67 proliferation index as a tool for chemotherapy decisions during and after neoadjuvant aromatase inhibitor treatment of breast cancer: Results from the American college of surgeons oncology group Z1031 trial (alliance). J Clin Oncol 35: 1061-1069, 2017.
22. Plant AL, Bhadriraju K, Spurlin TA and Elliott JT: Cell response to matrix mechanics: Focus on collagen. Biochim Biophys Acta 1793: 893-902, 2009.
23. Mak KM and Mei R: Basement membrane type IV collagen and laminin: An overview of their biology and value as fibrosis biomarkers of liver disease. Anat Rec (Hoboken) 300: 1371-1390, 2017.
24. Nugroho RWN, Harjumäki R, Zhang X, Lou YR, Yliperttula M, Valle-Delgado JJ and Österberg M: Quantifying the interactions between biomimetic biomaterials-collagen I, collagen IV, laminin 521 and cellulose nanofibrils-by colloidal probe microscopy. Colloids Surf B Biointerfaces 173: 571-580, 2019.
25. Koeck S, Zwierzina M, Lorenz E, Gamerith G, Zwierzina H and Amann A: Infiltration of immune cells into cancer cell/stroma cell 3D microtissues. J Immunother Cancer 3 (Suppl 2): P75, 2015.
26. Bray LJ, Binner M, Körner Y, von Bonin M, Bornhäuser M and Werner C: A three-dimensional ex vivo tri-culture model mimics cell-cell interactions between acute myeloid leukemia and the vascular niche. Haematologica 102: 1215-1226, 2017.
27. Bruce A, Evans R, Mezan R, Shi L, Moses BS, Martin KH, Gibson LF and Yang Y: Three-dimensional microfluidic tri-culture model of the bone marrow microenvironment for study of acute lymphoblastic leukemia. PLoS One 10: e0140506, 2015.
28. Liston DR and Davis M: Clinically relevant concentrations of anticancer drugs: A guide for nonclinical studies. Clin Cancer Res 23: 3489-3498, 2017.
29. Balaburski GM, Dardes RC, Johnson M, Haddad B, Zhu F, Ross EA, Sengupta S, Klein-Szanto A, Liu H, Lee ES, *et al*: Raloxifene-stimulated experimental breast cancer with the paradoxical actions of estrogen to promote or prevent tumor growth: A unifying concept in anti-hormone resistance. Int J Oncol 37: 387-398, 2010.
30. Brady H, Desai S, Gayo-Fung LM, Khammungkhune S, McKie JA, O'Leary E, Pascasio L, Sutherland MK, Anderson DW, Bhagwat SS and Stein B: Effects of SP500263, a novel, potent antiestrogen, on breast cancer cells and in xenograft models. Cancer Res 62: 1439-1442, 2002.
31. Schafer JM and Jordan VC: Models of hormone resistance in vitro and in vivo. Methods Mol Med 120: 453-464, 2006.
32. Azab SS, Salama SA, Hassan MH, Khalifa AE, El-Demerdash E, Fouad H, Al-Hendy A and Abdel-Naim AB: 2-Methoxyestradiol reverses doxorubicin resistance in human breast tumor xenograft. Cancer Chemother Pharmacol 62: 893-902, 2008.
33. Mansoori B, Mohammadi A, Davudian S, Shirjang S and Baradaran B: The different mechanisms of cancer drug resistance: A brief review. Adv Pharm Bull 7: 339-348, 2017.
34. Walter M, Liang S, Ghosh S, Hornsby PJ and Li R: Interleukin 6 secreted from adipose stromal cells promotes migration and invasion of breast cancer cells. Oncogene 28: 2745-2755, 2009.
35. Neiva KG, Warner KA, Campos MS, Zhang Z, Moren J, Danciu TE and Nör JE: Endothelial cell-derived interleukin-6 regulates tumor growth. BMC Cancer 14: 99, 2014.
36. Baghban R, Roshangar L, Jahanban-Esfahlan R, Seidi K, Ebrahimi-Kalan A, Jaymand M, Kolahian S, Javaheri T and Zare P: Tumor microenvironment complexity and therapeutic implications at a glance. Cell Commun Signal 18: 59, 2020.
37. Yamaguchi H and Sakai R: Direct interaction between carcinoma cells and cancer associated fibroblasts for the regulation of cancer invasion. Cancers (Basel) 7: 2054-2062, 2015.
38. Akino T, Hida K, Hida Y, Tsuchiya K, Freedman D, Muraki C, Ohga N, Matsuda K, Akiyama K, Harabayashi T, *et al*: Cytogenetic abnormalities of tumor-associated endothelial cells in human malignant tumors. Am J Pathol 175: 2657-2667, 2009.
39. Winkler J, Abisoye-Ogunniyan A, Metcalf KJ and Werb Z: Concepts of extracellular matrix remodelling in tumour progression and metastasis. Nat Commun 11: 5120, 2020.

40. Grigioni WF, Garbisa S, D'Errico A, Baccarini P, Stetler-Stevenson WG, Liotta LA and Mancini AM: Evaluation of hepatocellular carcinoma aggressiveness by a panel of extracellular matrix antigens. Am J Pathol 138: 647-654, 1991.
41. Nürnberg E, Vitacolonna M, Klicks J, von Molitor E, Cesetti T, Keller F, Bruch R, Ertongur-Fauth T, Riedel K, Scholz P, *et al*: Routine optical clearing of 3D-cell cultures: Simplicity forward. Front Mol Biosci 7: 20, 2020.
42. Imbalzano KM, Tatarkova I, Imbalzano AN and Nickerson JA: Increasingly transformed MCF-10A cells have a progressively tumor-like phenotype in three-dimensional basement membrane culture. Cancer Cell Int 9: 7, 2009.
43. Alessandri K, Sarangi BR, Gurchenkov VV, Sinha B, Kießling TR, Fetler L, Rico F, Scheuring S, Lamaze C, Simon A, *et al*: Cellular capsules as a tool for multicellular spheroid production and for investigating the mechanics of tumor progression in vitro. Proc Natl Acad Sci USA 110: 14843-14848, 2013.
44. Raghavan S, Mehta P, Horst EN, Ward MR, Rowley KR and Mehta G: Comparative analysis of tumor spheroid generation techniques for differential in vitro drug toxicity. Oncotarget 7: 16948-16961, 2016.
45. Loessner D, Stok KS, Lutolf MP, Hutmacher DW, Clements JA and Rizzi SC: Bioengineered 3D platform to explore cell-ECM interactions and drug resistance of epithelial ovarian cancer cells. Biomaterials 31: 8494-8506, 2010.
46. Karlsson H, Fryknäs M, Larsson R and Nygren P: Loss of cancer drug activity in colon cancer HCT-116 cells during spheroid formation in a new 3-D spheroid cell culture system. Exp Cell Res 318: 1577-1585, 2012.
47. Trédan O, Galmarini CM, Patel K and Tannock IF: Drug resistance and the solid tumor microenvironment. J Natl Cancer Inst 99: 1441-1454, 2007.
48. Barbosa MA, Xavier CP, Pereira RF, Petrikaite V and Vasconcelos MH: 3D cell culture models as recapitulators of the tumor microenvironment for the screening of anti-cancer drugs. Cancers (Basel) 14: 190, 2021.
49. Edmondson R, Broglie JJ, Adcock AF and Yang L: Three-dimensional cell culture systems and their applications in drug discovery and cell-based biosensors. Assay Drug Dev Technol 12: 207-218, 2014.
50. Yip D and Cho CH: A multicellular 3D heterospheroid model of liver tumor and stromal cells in collagen gel for anti-cancer drug testing. Biochem Biophys Res Commun 433: 327-332, 2013.
51. Benton G, DeGray G, Kleinman HK, George J and Arnaoutova I: In vitro microtumors provide a physiologically predictive tool for breast cancer therapeutic screening. PLoS One 10: e0123312, 2015.
52. Cornelison RC, Yuan JX, Tate KM, Petrosky A, Beeghly GF, Bloomfield M, Schwager SC, Berr AL, Cimini D, Bafakih FF, *et al*: A patient-designed tissue-engineered model of the infiltrative glioblastoma microenvironment. bioRxiv: Jul 29, 2020 (Epub ahead of print).
53. Wan X, Hou J, Liu S, Zhang Y, Li W, Zhang Y and Ding Y: Estrogen receptor α mediates doxorubicin sensitivity in breast cancer cells by regulating E-cadherin. Front Cell Dev Biol 9: 583572, 2021.
54. Halldorsson S, Lucumi E, Gómez-Sjöberg R and Fleming RM: Advantages and challenges of microfluidic cell culture in polydimethylsiloxane devices. Biosens Bioelectron 63: 218-231, 2015.
55. Ventola CL: Medical applications for 3D printing: Current and projected uses. P T 39: 704-711, 2014.
56. Marangoni E, Vincent-Salomon A, Auger N, Degeorges A, Assayag F, de Cremoux P, de Plater L, Guyader C, De Pinieux G, Judde JG, *et al*: A new model of patient tumor-derived breast cancer xenografts for preclinical assays. Clin Cancer Res 13: 3989-3998, 2007.
57. Cottu P, Marangoni E, Assayag F, de Cremoux P, Vincent-Salomon A, Guyader Ch, de Plater L, Elbaz C, Karboul N, Fontaine JJ, *et al*: Modeling of response to endocrine therapy in a panel of human luminal breast cancer xenografts. Breast Cancer Res Treat 133: 595-606, 2012.
58. Zhang X, Claerhout S, Prat A, Dobrolecki LE, Petrovic I, Lai Q, Landis MD, Wiechmann L, Schiff R, Giuliano M, *et al*: A renewable tissue resource of phenotypically stable, biologically and ethnically diverse, patient-derived human breast cancer xenograft models. Cancer Res 73: 4885-4897, 2013.
59. Fong EL, Martinez M, Yang J, Mikos AG, Navone NM, Harrington DA and Farach-Carson MC: Hydrogel-based 3D model of patient-derived prostate xenograft tumors suitable for drug screening. Mol Pharm 11: 2040-2050, 2014.